

Geophysical Research Letters

RESEARCH LETTER

10.1029/2021GL094679

Key Points:

- We simulate earthquake cycles in fault zones with coseismic damage and interseismic healing
- There are more surface-rupturing events with regular recurrence intervals as the modeled fault zones become more mature
- Healing in immature fault zone models promotes slow-slip events within the seismogenic zone causing partial ruptures

Supporting Information:

Supporting Information may be found in the online version of this article.

Correspondence to:

P. Thakur,
prith@umich.edu

Citation:

Thakur, P., & Huang, Y. (2021). Influence of fault zone maturity on fully dynamic earthquake cycles. *Geophysical Research Letters*, 48, e2021GL094679. <https://doi.org/10.1029/2021GL094679>

Received 7 JUN 2021
Accepted 17 AUG 2021

Influence of Fault Zone Maturity on Fully Dynamic Earthquake Cycles

Prithvi Thakur¹  and Yihe Huang¹ 

¹Department of Earth and Environmental Sciences, University of Michigan, Ann Arbor, MI, USA

Abstract We study the mechanical response of two-dimensional vertical strike-slip fault to coseismic damage evolution and interseismic healing of fault damage zones by simulating fully dynamic earthquake cycles. Our models show that fault zone structure evolution during the seismic cycle can have pronounced effects on mechanical behavior of locked and creeping fault segments. Immature fault damage zone models exhibit small and moderate subsurface earthquakes with irregular recurrence intervals and abundance of slow-slip events during the interseismic period. In contrast, mature fault damage zone models host pulse-like earthquake ruptures that can propagate to the surface and extend throughout the seismogenic zone, resulting in large stress drop, characteristic rupture extents, and regular recurrence intervals. Our results suggest that interseismic healing and coseismic damage accumulation in fault zones can explain the observed differences of earthquake behaviors between mature and immature fault zones and indicate a link between regional seismic hazard and fault structural maturity.

Plain Language Summary Fault zones are geometrically complex network of fractures with slip surfaces that are capable of hosting earthquakes. This network evolves through time as more and more earthquakes generate damage in the vicinity of the slip surfaces. We use numerical models to simulate different stages of fault-slip behavior including earthquakes, slow-slip events, and aseismic creep on a planar fault surrounded by a damage zone. This damage zone is prescribed to accumulate damage after an earthquake and heal during the quiet periods between earthquakes. Depending on the compliance (i.e., the ability to accommodate deformation) of the damage zone with respect to the surrounding host rock, a fault zone can be at different stages of its maturity, with higher compliance corresponding to a more mature fault zone. We find that our models with immature fault zone tends to produce smaller earthquakes whose slip does not reach the surface of the earth, and the duration between earthquakes is irregular. As fault zones become more mature in the models, earthquakes can rupture to the surface and occur more regularly. Our results highlight a link between regional seismic hazard and fault structural maturity.

1. Introduction

Active faults are usually surrounded by narrow regions of localized deformation extending several hundred meters to a few kilometers in width across the fault. This deformation zone consisting of a dense fracture network is macroscopically viewed as an elastic layer with low-seismic wave velocities and referred to as a fault damage zone (Ben-Zion & Sammis, 2003). The strength of the fault damage zone evolves throughout the seismic cycle, but the details of the evolution mechanism and the nature of this evolution remain elusive.

Fault zone maturity can be defined and quantified by the total slip accumulated over time in field geologic and geodetic studies (Dolan & Haravitch, 2014), with larger slip corresponding to higher maturity. Figure 1 shows a conceptual model of how a strike-slip fault system may evolve through multiple earthquake cycles. Immature fault zones (Figure 1a) are characterized by a distributed network of damage, and as the fault zone matures (Figure 1c), the damage becomes localized. The faulting itself becomes more localized, transitioning from multiple and discontinuous slip surfaces to a more throughgoing fault. Other parameters such as the total fault length, the slip rate, and the initiation age have also been used to determine fault zone maturity (Perrin et al., 2016). However, the surface slip expression for immature faults usually underestimate slip at depth by about 10%–60% (Dolan & Haravitch, 2014). Perrin et al. (2016) have shown that structural maturity of a strike-slip fault zone is well correlated with the seismic wave velocity of near-fault

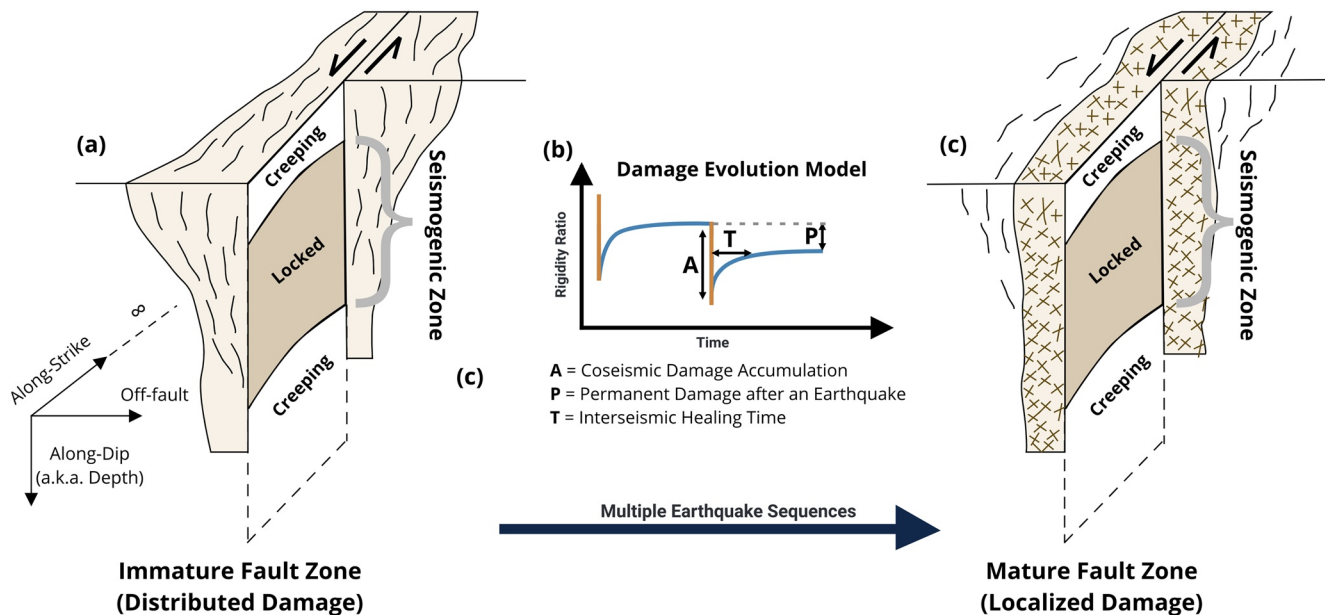


Figure 1. A conceptualized evolution of a fault damage zone through multiple earthquake sequences for strike-slip fault systems. (a) Schematic of an immature fault zone with distributed damage increases toward the surface. (b) Parameters considered for an elastic damage evolution model, showing the prescribed change in the rigidity ratio (ratio of shear modulus in damage zone to that in the host rock) through time. (c) Schematic of a mature fault zone with localized damage and a dense fracture network.

materials, which decreases as the fault zone becomes progressively more mature. Such velocity reductions are well documented along mature fault zones such as the San Andreas fault zone (Y.-G. Li et al., 2006; Lewis & Ben-Zion, 2010), San Jacinto fault zone (Lewis et al., 2005), Nojima fault zone (Mizuno et al., 2008), and Wenchuan fault zone (Pei et al., 2019). Examples of immature fault zones that exhibit less evidence of localized damage include the northern part of the San Andreas fault zone (Waldhauser & Ellsworth, 2002), the Bam fault in Iran (Fielding et al., 2009), the Jiuzhaigou earthquake near Kunlun fault zone in China (Y. Li et al., 2020), and Peloponnese fault zone in Greece (Feng et al., 2010). Previous studies have shown that a more compliant or mature fault damage zone enables ruptures to propagate as slip pulses (Harris & Day, 1997; Huang & Ampuero, 2011; Huang et al., 2014; Idini & Ampuero, 2020a, 2020b; Thakur et al., 2020). Geodetic observations (e.g., Feng et al., 2010; Goldberg et al., 2020) have shown earthquake slip distributions are complex in an immature fault zone, and they become more uniform as the fault zone matures. Understanding the long-term earthquake behavior during the structural evolution of the fault damage zone is key to unraveling the locations, recurrence intervals, stressing history, and the probability of subsequent earthquakes in an active fault zone.

Observations of seismic wave velocity changes within the fault damage zone (<1 km from the fault; e.g., Y.-G. Li et al., 2003, 2006; Peng & Ben-Zion, 2006; Roux & Ben-Zion, 2014; Vidale & Li, 2003; Wu et al., 2009; Zhao & Peng, 2009) documented a sharp decrease in pressure- and shear-wave velocities following earthquakes as well as a subsequent logarithmic increase in wave velocity with time. Other observations further away from the fault zone (e.g., Chen et al., 2015; Pei et al., 2019; Taira et al., 2009) revealed coseismic reduction and interseismic increase of seismic wave velocities in the surrounding region. Laboratory experiments have shown similar change in seismic wave velocities (Johnson & Jia, 2005; Kaproth & Marone, 2014; Snieder et al., 2016) wherein they observe compaction during holds (i.e., interseismic period) and dilation during fault slip (i.e., seismic events). Mechanisms for damage accumulation in active fault zones are likely a combination of processes including dilation, compaction, cracking, shear driven pulverization, and fabric generation (Gratier et al., 2003). The observed coseismic seismic velocity drop is potentially related to brecciation, cataclasis, and damage accumulation, implying a magnitude dependence of this velocity drop (Brenugier et al., 2008; Y.-G. Li et al., 2003; Rubinstein & Beroza, 2005).

During the interseismic period, time-dependent fault zone healing may occur due to a combination of rheological restrengthening, inelastic strain, mineral precipitation, and fluid pressure recovery (Vidale & Li, 2003). There is some debate on whether this healing time is significant in contributing to fault zone stress redistribution and therefore influencing long-term seismicity (Mizuno et al., 2008; Vidale & Li, 2003). It is hard to accurately quantify fault zone healing time because it requires long-term continuous monitoring of seismic wave velocities. Active seismic studies along the Landers fault zone (Vidale & Li, 2003) and Longmenshan fault zone (Pei et al., 2019) suggest that it may take years or decades to heal completely, whereas other studies (Mizuno et al., 2008; Peng & Ben-Zion, 2006; Wu et al., 2009) suggest that the healing time may not be longer than the typical timescales of postseismic afterslip, that is, a couple of months. Another study by Roux and Ben-Zion (2014) along the North Anatolian Fault suggests a recovery rate over a timescale of few days. It is worthwhile noting that some of these studies may have a lower spatial resolution than others which might affect the inference of fault zone recovery rate.

We use numerical simulations to understand the effects of fault zone damage accumulation after multiple cycles of earthquakes and healing during the interseismic period on a two-dimensional (2D) vertical strike-slip fault. We model the fault zone structure evolution as changes in the shear-wave velocity of an elastic layer surrounding a strike-slip fault. This elastic fault damage zone has a lower shear-wave velocity, and therefore, a lower rigidity compared to the surrounding host rock. We assume a constant density in our numerical simulations as the changes in shear-wave velocity has a more significant effect on the rigidity of the material. Throughout the remainder of this article, we will use the term “rigidity ratio,” which is the percentage ratio of the fault zone shear modulus to the host rock shear modulus, to parameterize the fault zone evolution through time. Figure 1b shows a representative rigidity ratio evolution through time. We constrain the coseismic damage accumulation and the rate of interseismic healing using shear-wave velocity observations from Wenchuan (Pei et al., 2019), Landers (Vidale & Li, 2003), Nojima (Mizuno et al., 2008), and North Anatolian Fault zones (Peng & Ben-Zion, 2006). We describe the numerical procedure and the fault zone healing mechanism in Section 2 and Supporting Information S1. The results of our models are described in Section 3. We show that an immature fault zone tends to produce more slow-slip events and irregular earthquake sequences with predominantly subsurface events. In contrast, a more mature fault damage zone tends to produce a more regular sequence of earthquakes with a combination of surface-reaching and subsurface events. In Section 4, we discuss the implications of our results for earthquake cycle behaviors of strike-slip fault zones.

2. Model Description

We use 2D earthquake cycle models of strike-slip faults with mode III rupture where the displacement is out of the plane of interest and stresses and friction vary with depth. For simplicity, we use a narrow fault-parallel layer as a proxy for the damage zone and its geometry remains constant throughout the simulated sequence. This is equivalent taking a vertical cross-section across Figure 1c, and the fault zone maturity in the damage evolution model corresponds to the change in rigidity ratio without changing the geometry of the fault zone (Figure 1b). The frictional properties and initial conditions are chosen to keep the frictional complexities at a minimum (see Supporting Information S1). Here, we focus the discussion on-fault zone properties.

Since there are very few long-term observations (10,000–100,000 years) documenting the changes in permanent damage through multiple earthquake cycles, we limit ourselves to modeling short earthquake sequences for several hundred years each, with each sequence intended to represent different stages of fault zone maturity, including an immature stage and a mature stage, both of which accumulate no permanent damage. We also consider a transition stage which incorporates permanent damage, that is, a reduction in rigidity after each earthquake. The distinction between immature and mature fault zones in our models depends on the rigidity ratio of the damage zone to the host rock. Typically, larger velocity reductions (35%–50%) and lower rigidities (25%–45% of host rock) are measured around mature fault zones, whereas smaller velocity reductions (8%–10%) and higher rigidities (80%–90% of host rock) are measured around immature fault zones (Perrin et al., 2016). Based on these seismic wave velocity measurements, we choose a rigidity ratio changing between 80% and 85% of host rock for the immature fault zone and a rigidity ratio changing

between 40% and 45% of the host rock for the mature fault zone. While mature fault zones can have lower rigidities as well, the chosen values lie well within what is observed for mature and immature fault zones.

Another important parameter is the coseismic velocity drop. While its value is not well constrained by observations and can vary significantly (0.1%–5%) between different fault zones such as Parkfield (Y.-G. Li et al., 2006), Wenchuan (Pei et al., 2019), and Landers (Y.-G. Li et al., 2003), it is dependent on the size of the earthquake with smaller earthquakes showing smaller coseismic drop. Since our simulations are 2D and do not have any along-strike constraints on the earthquake size, we use a magnitude-independent coseismic damage accumulation of 5% rigidity change in order to facilitate a better comparison between different simulation cycles.

Our current models are a purely elastic approximation of how a fault damage zone may evolve over time through multiple earthquake sequences. This ignores the energy dissipated through the damage process (e.g., Okubo et al., 2019), including that required for secondary crack formation (Lyakhovskiy et al., 2005). Additionally, the coseismic velocity drop in our models approximates the damage evolution and crack propagation over smaller timescales during each event to a step change that occurs after the event is over. Other plausible mechanisms such as fault roughness evolution (Heimisson, 2020), or alternate modeling approaches such as elastic impact (Tsai & Hirth, 2020) might influence the dynamics of earthquake sequences. While incorporating these complexities may affect the overall fault-slip behavior, they are computationally very expensive to implement and beyond the scope of the current study.

3. Results

We have tested a range of parameters in our simulations that account for fault zone maturity, coseismic damage accumulation, and healing time. Here the fault zone maturity can be described by the initial rigidity ratio (Figure 1b). These parameters are discussed in Supporting Information S1. For brevity, we choose to show representative cases for a healing time of 8 years and a coseismic velocity drop of 5% in the following subsections. Changing these parameters (e.g., healing time between 1 and 20 years) have some effects on the location and timing of individual earthquakes but does not affect the overall interpretation of our results.

3.1. Effects of Fault Damage Zone Maturity

The initial rigidity ratio of fault damage zones with respect to the surrounding host rock can have significant effects on seismicity evolution. A higher initial rigidity ratio implies a less mature fault zone and vice versa. While keeping the permanent damage at zero, we compare an immature fault zone evolution characterized by rigidity ratio changing between 80% and 85%, against a mature fault zone evolution characterized by rigidity ratio changing between 40% and 45% (Figures 2a and 2b). For the sake of simplicity, the fault zone accumulates damage by the same amount irrespective of the earthquake size.

For the models with a constant healing time, a mature fault zone tends to show more regular earthquake sequences with full (surface-reaching) ruptures, whereas a less mature fault zone shows irregular earthquake sequences with partial (subsurface) ruptures and more slow-slip events (Figures 2c and 2d). The cumulative slip demonstrates events with variable sizes and depths throughout the seismogenic zone, but we do not see ruptures spanning the entire seismogenic region in the immature fault zone. Instead, we only see ruptures extending across a fraction of the seismogenic zone, and these partial ruptures persist throughout multiple seismic cycles. This phenomenon of partial ruptures occurs only in immature fault zone model with healing, which tend to have crack-like ruptures and overall lower slip velocities. In contrast, mature fault zone model exhibit higher slip velocities and pulse-like ruptures, which tend to produce surface-reaching ruptures. Such pulse-like ruptures can be identified by looking at the cumulative slip of earthquake cycles in mature fault zones (Figure 2d), where the final slip distribution is nearly flat, a characteristic of pulse-like ruptures (Heaton, 1990).

We measure shear stress before and after a representative earthquake from each of these simulations to understand the depth distribution of stress drop and the mechanisms accounting for different earthquake behaviors in mature and immature fault zones. Figures 2e and 2f show the depth distribution of shear stress for an earthquake in the immature and mature fault zone models, respectively. We see that the mature fault

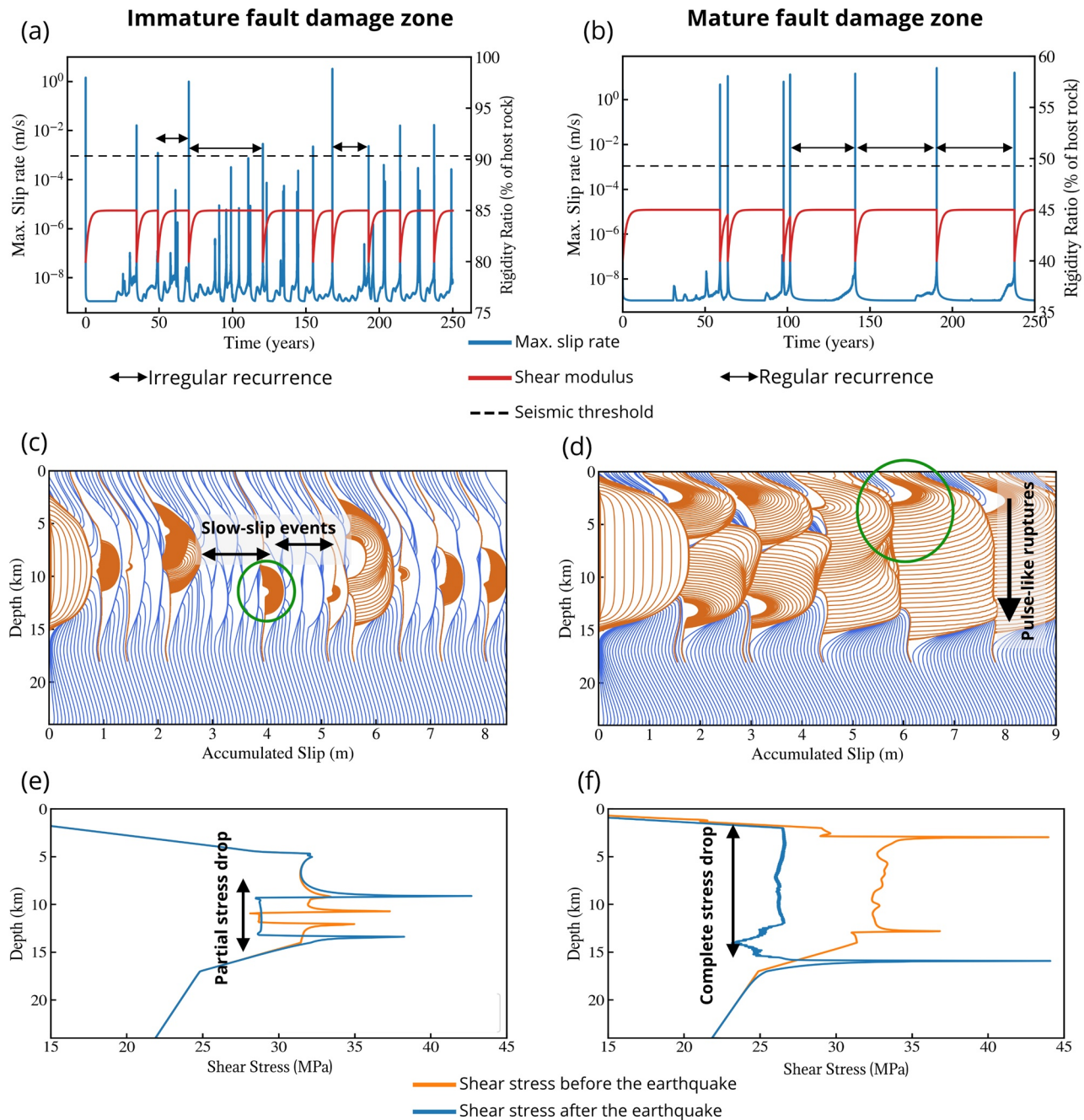


Figure 2. Immature versus mature fault damage zone. (a and b) The evolution of slip-rate function (blue) and the rigidity ratio (red) through time. (c and d) Cumulative slip through earthquake sequences shown along depth in mature and immature fault zones. The orange lines are plotted every 0.1 s during earthquakes, and the blue lines are plotted every year during interseismic periods. (e and f) The on-fault shear stress before and after a representative earthquake for each case (circled in green in [c] and [d]) demonstrates a partial stress drop for immature fault zones and a complete stress drop for mature fault zones.

zone model exhibits a large, uniform stress drop along the fault dip (Figure 2f) such that stress peaks after the earthquake are concentrated only toward the edges of the velocity-weakening segment due to ruptures propagating throughout the seismogenic zone. On the other hand, the immature fault zone model (Figure 2e) results in a partial stress drop as the rupture is arrested before reaching the edges of the asperity. In this context, a partial stress drop refers to the stresses being released only in a small portion of the velocity-weakening segment along the fault. The partial stress drop in immature fault zones leads to residual

stress peaks concentrated within the velocity-weakening region, which may cause subsequent ruptures or slow-slip events near those stress peaks. As discussed in more detail in Section 3.2, the slow-slip events can delay the next earthquake rupture and result in irregular recurrence intervals between earthquakes.

We also include permanent damage after each earthquake in our model to demonstrate the transition from an immature fault zone to a mature fault zone (i.e., P is nonzero in Figure 1b). While faults in nature need several tens of thousands of years to transition from immature to mature stages, it is not computationally feasible to perform such simulations with full inertial effects. The choice of the amount of coseismic velocity reduction and interseismic healing in our simulations allows the transition from immature to mature fault zones within 300–400 years. Figure S1 shows the accumulated slip contours for the earthquake cycle in this scenario. We begin with an initial rigidity ratio of 90% and drop it down by 5% after each earthquake (Figure S1). We allow the fault to recover 80% of the coseismic drop in rigidity during the interseismic period therefore accommodating a permanent damage of 1% rigidity reduction after each earthquake, though smaller recovery percentages may be achieved if the next earthquake occurs before the fault has healed completely (Figure S1b). We see a progressive increase in the rupture length from partial to full ruptures as the fault zone becomes more mature (Figure S1a). We distinguish between an immature and a mature fault damage zone based on when we start observing surface-reaching events that rupture the entire seismogenic zone. Surface-reaching ruptures become prevalent when the rigidity ratio falls below 60% of the host rock. Furthermore, earthquakes become more regular and frequent as the fault zone matures. This simulation informs us that the transition from immature to mature fault zone is gradual, and we can see a mixture of surface-reaching and subsurface events during this transition stage.

3.2. Effects of Healing: Slow-Slip Events and Irregularity in Recurrence Intervals

Interseismic healing has significant effects on the dynamics of earthquakes and aseismic fault-slip, including creep accumulation within the nominally velocity-weakening region, inhibition of surface-reaching events, restriction of earthquake sizes, and generation of slow-slip events also within the velocity-weakening region. Here we discuss the effects of healing in an immature fault zone in more detail and demonstrate how slow-slip events affect seismicity by comparing a simulation with fault zone rigidity ratio ranging between 60% and 65% against a fault zone with the same initial rigidity ratio but without healing (i.e., a constant rigidity ratio of 60%). This range of rigidity ratio still lies in the immature fault zone parameter space discussed in the previous section but leads to fewer slow-slip events compared to the 80%–85% range. It allows us to analyze the healing effect and slow-slip events more clearly.

In our numerical simulations, slow-slip events are manifested as accelerated slip that fail to reach the seismic threshold velocity but release finite stress on the slip patch along a portion of the fault. The slip rate of slow-slip events in our simulations can vary from 1×10^{-8} to 1×10^{-4} m s⁻¹ (Figure 3). Besides slow-slip events, the events below the seismic threshold in our simulations also encompass aseismic creep and afterslip (Figure 3b). Aseismic creep is characterized by slip rate that is close to the tectonic plate rate ($\leq 1 \times 10^{-9}$ m s⁻¹). Afterslip is another category of transient slow-slip that releases stresses from recent earthquakes during the postseismic stage (Avouac, 2015; Bürgmann, 2018). The slip rate of afterslip is typically below the seismic slip rate of 1 mm s⁻¹ and can go down to 1×10^{-5} m s⁻¹. Afterslip can be distinguished from the slow-slip events by when and where they occur, that is, away from peak-slip regions of earthquakes.

Figures 3a and 3b show the slip-rate evolution for a fault zone without and with healing during the seismic cycle. The simulation without healing (Figure 3a) shows large surface-reaching ruptures that are periodic in time. This sequence of earthquakes encompasses dynamic events and aseismic creep but does not exhibit any slow-slip events between them. Figure 3b shows a wider range of events including multiple slow-slip events in addition to earthquakes and creep. Such slow-slip events can be identified from the peak-slip rate function in these simulations (Figures 2a, 2b, and 3d) and generally occur during the interseismic stage within the seismogenic zone in our simulations (Figures 3b and 3d). These slow-slip events are distributed throughout the interseismic period, with no temporal preference before or after an earthquake, though they have a spatial preference in relation to the residual stresses from previous events. Earthquake ruptures and slow-slip events in our simulations with fault zone healing occur at the edges of previous ruptured region within the velocity-weakening zone (Figure 3b), due to residual stress peaks from those events. The slow-slip events also contribute to the release of stresses during the interseismic period, and in addition, generate

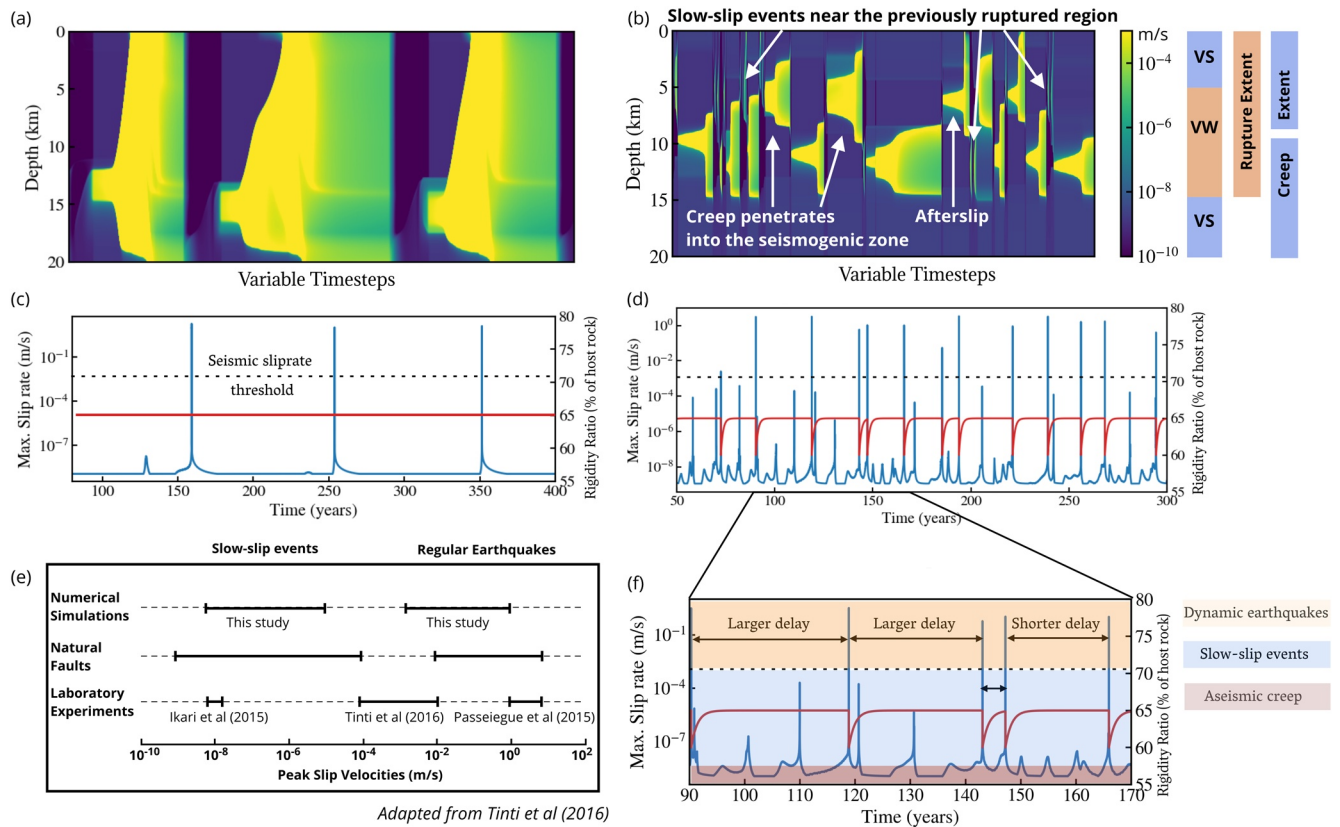


Figure 3. (a) The spatiotemporal slip-rate evolution in immature fault zone without healing (see color scale in [b]). (b) The spatiotemporal slip-rate evolution in immature fault zone with healing. The right side shows the depth extent of the frictional parameters delineating the velocity-weakening and the velocity-strengthening region. (c and d) The rigidity ratio and the peak-slip rate function for a segment of the simulation. (e) A compilation of the peak-slip-velocity range for slow-slip events from laboratory experiments, natural faults, and our numerical simulations. (f) Zoom in of part (d), showing larger delay in earthquake onset for higher slow-slip rates.

stress peaks within the seismogenic zone, away from its base. This is in contrast to the simulation without healing (Figure 3a), where the stress peaks are predominantly near the base of the seismogenic zone. Other numerical studies (Barbot, 2019b; Idini & Ampuero, 2020a, 2020b) also showed that slow-slip events can be generated in the velocity-weakening part of the fault using quasi-dynamic continuum models. However, the relative size of seismogenic asperity to nucleation, R_u (Barbot, 2019b), for such simulations is much lower than what we use here. Such numerical simulations can exhibit periodic slow-slip events at lower R_u values (<1) and chaotic slow-slip events at higher R_u values (>13). Our simulations use an $R_u \sim 5$, which should result in periodic bilateral ruptures, as seen in Figure 3a. Note that the incorporation of healing does not change the R_u values significantly as they lie in the same parameter regime through time. However, interseismic healing helps release the stresses inelastically through time during the quasi-static deformation, which rearranges the stress peaks and stress shadows along the fault dip, resulting in restriction of earthquake sizes and generation of slow-slip events.

Since the interseismic healing promotes slow-slip events, stresses are released nonuniformly along the fault during this period. This causes partial ruptures to terminate without reaching the free surface. Moreover, these slow-slip events delay the onset of subsequent earthquakes. We see in Figures 3d and 3f that earthquakes become farther apart in time when there are slow-slip events between them, as compared to consecutive earthquakes occurring without such slow-slip events. This delay, combined with the occurrence of slow-slip events within the velocity-weakening region, gives rise to the irregular recurrence of earthquakes in immature fault zones with healing. We can also infer that the slow-slip events with higher amount of slip release more stresses during the interseismic period, which delays the subsequent earthquake by a larger amount (Figure 3f).

Another notable feature of the simulation with healing is the penetration of aseismic creep into the velocity-weakening part of the fault (Figure 3b). The simulation without healing (Figures 3a and 3c) shows complete ruptures with regular recurrence intervals, and aseismic creep is constrained to the velocity-strengthening parts of the fault. However, the incorporation of healing during the interseismic period allows the creep to accumulate and build up progressively within the velocity-weakening region (Figures 3b and 3d). We demonstrate the cumulative rupture and creep extent from all the events in our simulation with healing in relation to the velocity-weakening and velocity-strengthening regions along the fault on the right side of Figure 3b. We see that the cumulative creep extends through almost the entire fault, whereas the earthquake rupture extent is predominantly confined to the velocity-weakening region. Creeping within the seismogenic zone also causes nonuniform stress release during the interseismic period, similar to the effects of slow-slip events discussed above, albeit to a lesser extent.

This effect of creep buildup within the velocity-weakening region and the abundance of slow-slip events is also observed in our simulation with permanent damage (Figure S1). We observe more slow-slip events during the immature stage of the fault zone which is responsible for irregular recurrence intervals for earthquakes. These slow-slip events become less frequent during the mature stages of the earthquake cycle, and thus there is a more regular sequence of earthquakes. This transition is in accordance with the results from the previous section highlighting the differences between a mature and immature fault damage zone without permanent damage. We show the slip-rate range of slow-slip events and fast earthquakes in our simulations, in comparison to those observed on natural faults and in laboratory experiments in Figure 3e. We see that our numerical simulation of a fault zone with healing can produce a wide range of events, both in the fast slipping and slow slipping regime, comparable to those observed along natural faults.

4. Discussions and Conclusions

Seismologic and geodetic observations in immature fault zones exhibit complex ruptures and distributed coseismic damage. The damage zones in these faults are wider with poorly defined boundaries, resulting in earthquake sequences exhibiting irregular recurrence and size distributions akin to a Gutenberg-Richter magnitude scaling. Examples of such fault zones include the Ridgecrest sequence where geodetic studies have shown complex, multi-fault, and slow rupture with a heterogeneous static stress change (Goldberg et al., 2020). The study by DuRoss et al. (2016) along the immature Wasatch fault zone in Utah suggests partial-segment and multi-segment ruptures with irregular recurrence intervals. Seismic studies after the 2008 earthquake in Peloponnese, Greece have shown negligible surface deformation, that is, a coseismic slip deficit toward the surface (Feng et al., 2010; Fielding et al., 2009). Dolan and Haravitch (2014) compiled multiple fault zone studies to show that the ratio of the surface slip-measurements to the slip at depth is correlated with fault zone maturity, and immature fault zones tend to have lower ratios. These studies imply that immature fault zones lack surface slip during the coseismic phase and exhibit irregular recurrence intervals, which is also corroborated by our models. In contrast, very mature sections of fault zones have been shown to exhibit higher regularity in earthquake recurrence (e.g., Apline fault in Berryman et al., 2012; Howarth et al., 2021).

Our results unveil how the seismic and aseismic segments in a fault zone interact during the earthquake cycle within an elastic framework. We have shown that the seismogenic zone (velocity-weakening) in our models can have both seismic and aseismic slip episodes, with the latter encompassing slow-slip and creep events. The slow-slip events in our models are distributed within the velocity-weakening segment of the fault and occur throughout the interseismic period. Additionally, we see the aseismic creep penetrating into the velocity-weakening region in our immature fault zone models with healing. Both phenomena contribute to the nonuniform release of stresses during the seismic cycle, with slow-slip events having a dominant effect on the earthquake recurrence. Slow-slip events are very challenging to observe in geologically immature strike-slip faults using seismic or geodetic methods. Certain observations along strike-slip fault zones (e.g., the Northern SAF in Murray et al. (2014)) and subduction zones (e.g., Japan subduction zone in Johnson et al., 2016) have shown seismic and aseismic slip episodes occurring in the nominally velocity-weakening region. As subduction zones tend to be old and mature, some local geologic structures like heterogeneous seafloor structure or complex material properties associated with partially coupled subduction zone might be needed to rejuvenate them (Wang & Bilek, 2014). Surface creep has been observed on

several fault systems including the Maacama and Bartlett Springs (McFarland et al., 2009; Tong et al., 2013), and creep rates in the shallow parts can be locally very high in the order of 1×10^{-6} to 1×10^{-9} m s⁻¹ (Murray et al., 2014). This creep is suggested to extend to depths overlapping with some or all of the seismogenic zone in the Northern San Andreas fault system (Murray et al., 2014). Bruhat and Segall (2017) have explored models where they discuss that the updip propagation of deep interseismic creep can explain the slip-rate profile along the Northern Cascadia subduction zone. These creep episodes may allude to slow-slip events happening in these regions of immature fault zones as well as subduction zones. Such conditions would be expected to extend the time between major earthquakes, and potentially also limit the earthquake size.

To summarize, we performed fully dynamic earthquake cycle simulations in a 2D strike-slip fault surrounded by an elastic damage zone with time-dependent shear modulus evolution that emulates coseismic damage and interseismic healing during seismic and aseismic periods respectively. The models with interseismic healing in immature fault zones can promote aseismic slip episodes including slow-slip events and creep to propagate into the seismogenic zone. Our numerical simulations show that such events in immature fault zones can limit the size of earthquakes and prolong the time between large earthquakes. In these simulations, slow-slip events are abundant and the stress peaks from previous earthquakes and slow-slip events are critical in determining the location of and timing of subsequent events, thereby creating irregularity in recurrence intervals and partial ruptures. These partial ruptures lead to predominantly subsurface events in immature fault zones. In contrast, the higher compliance of mature fault zones leads to earthquakes with complete stress drops and rupture extending throughout the seismogenic zone. We demonstrate that such fundamental variations in fault-slip behavior can arise due to how the fault zone structure evolves in time, despite using simple elastic damage zone rheology and frictional fault properties. Our results emphasize the importance of monitoring seismic wave velocities and interseismic healing along active faults to help better characterize their first-order mechanical behavior.

Data Availability Statement

The code used to perform all the numerical simulations are available at: <https://zenodo.org/record/4898347>. It is citeable as: “Prithvi Thakur. (2021, June 3). thehalfspace/Sphear: (Version v1.0.0). Zenodo. <https://doi.org/10.5281/zenodo.4898347>”.

Acknowledgments

This study was supported by the National Science Foundation (Grant Award EAR-1943742) and Southern California Earthquake Center (Contribution number 20091). The authors thank the editor Dr. German Prieto, the associate editor Dr. Victor Tsai, and the two anonymous reviewers for their helpful comments. The authors thank Dr. Roland Burgmann and Dr. Yoshihiro Kaneko for helpful discussions that significantly improved the quality of this manuscript.

References

- Avouac, J.-P. (2015). From geodetic imaging of seismic and aseismic fault slip to dynamic modeling of the seismic cycle. *Annual Review of Earth and Planetary Sciences*, 43, 233–271. <https://doi.org/10.1146/annurev-earth-060614-105302>
- Barbot, S. (2019b). Slow-slip, slow earthquakes, period-two cycles, full and partial ruptures, and deterministic chaos in a single asperity fault. *Tectonophysics*, 768, 228171. <https://doi.org/10.1016/j.tecto.2019.228171>
- Ben-Zion, Y., & Sammis, C. G. (2003). Characterization of fault zones. *Pure and Applied Geophysics*, 160(3–4), 677–715. https://doi.org/10.1007/978-3-0348-8010-7_11
- Berryman, K. R., Cochran, U. A., Clark, K. J., Biasi, G. P., Langridge, R. M., & Villamor, P. (2012). Major earthquakes occur regularly on an isolated plate boundary fault. *Science*, 336(6089), 1690–1693. <https://doi.org/10.1126/science.1218959>
- Brenguier, F., Campillo, M., Hadziioannou, C., Shapiro, N. M., Nadeau, R. M., & Larose, E. (2008). Postseismic relaxation along the San Andreas Fault at Parkfield from continuous seismological observations. *Science*, 321(5895), 1478–1481. <https://doi.org/10.1126/science.1160943>
- Bruhat, L., & Segall, P. (2017). Deformation rates in northern Cascadia consistent with slow updip propagation of deep interseismic creep. *Geophysical Journal International*, 211(1), 427–449. <https://doi.org/10.1093/gji/ggx317>
- Bürgmann, R. (2018). The geophysics, geology and mechanics of slow fault slip. *Earth and Planetary Science Letters*, 495, 112–134. <https://doi.org/10.1016/j.epsl.2018.04.062>
- Chen, K. H., Furumura, T., & Rubinstein, J. (2015). Near-surface versus fault zone damage following the 1999 Chi-Chi earthquake: Observation and simulation of repeating earthquakes. *Journal of Geophysical Research: Solid Earth*, 120(4), 2426–2445. <https://doi.org/10.1002/2014JB011719>
- Dolan, J. F., & Haravitch, B. D. (2014). How well do surface slip measurements track slip at depth in large strike-slip earthquakes? The importance of fault structural maturity in controlling on-fault slip versus off-fault surface deformation. *Earth and Planetary Science Letters*, 388, 38–47. <https://doi.org/10.1016/j.epsl.2013.11.043>
- DuRoss, C. B., Personius, S. F., Crone, A. J., Olig, S. S., Hylland, M. D., Lund, W. R., & Schwartz, D. P. (2016). Fault segmentation: New concepts from the Wasatch Fault Zone, Utah, USA. *Journal of Geophysical Research: Solid Earth*, 121(2), 1131–1157. <https://doi.org/10.1002/2015JB012519>
- Feng, L., Newman, A. V., Farmer, G. T., Psimoulis, P., & Stiros, S. C. (2010). Energetic rupture, coseismic and post-seismic response of the 2008 M_w 6.4 Achaia-Elia Earthquake in northwestern Peloponnese, Greece: An indicator of an immature transform fault zone. *Geophysical Journal International*, 183(1), 103–110. <https://doi.org/10.1111/j.1365-246X.2010.04747.x>

- Fielding, E. J., Lundgren, P. R., Bürgmann, R., & Funning, G. J. (2009). Shallow fault-zone dilatancy recovery after the 2003 bam earthquake in Iran. *Nature*, 458(7234), 64–68. <https://doi.org/10.1038/nature07817>
- Goldberg, D. E., Melgar, D., Sahakian, V. J., Thomas, A. M., Xu, X., Crowell, B. W., & Geng, J. (2020). Complex rupture of an immature fault zone: A simultaneous kinematic model of the 2019 Ridgecrest, CA Earthquakes. *Geophysical Research Letters*, 47(3), e2019GL086382. <https://doi.org/10.1029/2019GL086382>
- Gratier, J.-P., Favreau, P., & Renard, F. (2003). Modeling fluid transfer along California faults when integrating pressure solution crack sealing and compaction processes. *Journal of Geophysical Research*, 108(B2). <https://doi.org/10.1029/2001JB000380>
- Harris, R. A., & Day, S. M. (1997). Effects of a low-velocity zone on a dynamic rupture. *Bulletin of the Seismological Society of America*, 87(5), 1267–1280.
- Heaton, T. H. (1990). Evidence for and implications of self-healing pulses of slip in earthquake rupture. *Physics of the Earth and Planetary Interiors*, 64(1), 1–20. [https://doi.org/10.1016/0031-9201\(90\)90002-F](https://doi.org/10.1016/0031-9201(90)90002-F)
- Heimisson, E. R. (2020). Crack to pulse transition and magnitude statistics during earthquake cycles on a self-similar rough fault. *Earth and Planetary Science Letters*, 537, 116202. <https://doi.org/10.1016/j.epsl.2020.116202>
- Howarth, J. D., Barth, N. C., Fitzsimons, S. J., Richards-Dinger, K., Clark, K. J., Biasi, G. P., et al. (2021). Spatiotemporal clustering of great earthquakes on a transform fault controlled by geometry. *Nature Geoscience*, 14(5), 314–320. <https://doi.org/10.1038/s41561-021-00721-4>
- Huang, Y., & Ampuero, J.-P. (2011). Pulse-like ruptures induced by low-velocity fault zones. *Journal of Geophysical Research*, 116(B12). <https://doi.org/10.1029/2011JB008684>
- Huang, Y., Ampuero, J.-P., & Helmberger, D. V. (2014). Earthquake ruptures modulated by waves in damaged fault zones. *Journal of Geophysical Research: Solid Earth*, 119(4), 3133–3154. <https://doi.org/10.1002/2013jb010724>
- Idini, B., & Ampuero, J.-P. (2020a). Fault-zone damage promotes pulse-like rupture and back-propagating fronts via quasi-static effects. *Geophysical Research Letters*, 47(23), e2020GL090736. <https://doi.org/10.1029/2020GL090736>
- Idini, B., & Ampuero, J.-P. (2020b). *Fault-zone damage promotes pulse-like rupture and rapid-tremor-reversals*.
- Johnson, K. M., Mavrommatis, A., & Segall, P. (2016). Small interseismic asperities and widespread aseismic creep on the northern Japan subduction interface. *Geophysical Research Letters*, 43(1), 135–143. <https://doi.org/10.1002/2015GL066707>
- Johnson, P. A., & Jia, X. (2005). Nonlinear dynamics, granular media and dynamic earthquake triggering. *Nature*, 437(7060), 871–874. <https://doi.org/10.1038/nature04015>
- Kaproph, B. M., & Marone, C. (2014). Evolution of elastic wave speed during shear-induced damage and healing within laboratory fault zones. *Journal of Geophysical Research: Solid Earth*, 119(6), 4821–4840. <https://doi.org/10.1002/2014JB011051>
- Lewis, M. A., & Ben-Zion, Y. (2010). Diversity of fault zone damage and trapping structures in the Parkfield section of the San Andreas Fault from comprehensive analysis of near fault seismograms. *Geophysical Journal International*, 183(3), 1579–1595. <https://doi.org/10.1111/j.1365-246x.2010.04816.x>
- Lewis, M. A., Peng, Z., Ben-Zion, Y., & Vernon, F. (2005). Shallow seismic trapping structure in the San Jacinto fault zone near Anza, California. *Geophysical Journal International*, 162(3), 867–881. <https://doi.org/10.1111/j.1365-246x.2005.02684.x>
- Li, Y., Bürgmann, R., & Zhao, B. (2020). Evidence of fault immaturity from shallow slip deficit and lack of postseismic deformation of the 2017 Mw 6.5 Jiuzhaigou Earthquake. *Bulletin of the Seismological Society of America*, 110(1), 154–165. <https://doi.org/10.1785/0120190162>
- Li, Y.-G., Chen, P., Cochran, E. S., Vidale, J. E., & Burdette, T. (2006). Seismic evidence for rock damage and healing on the San Andreas Fault associated with the 2004 M 6.0 Parkfield earthquake. *Bulletin of the Seismological Society of America*, 96(4B), S349–S363. <https://doi.org/10.1785/0120050803>
- Li, Y.-G., Vidale, J. E., Day, S. M., Oglesby, D. D., & Cochran, E. (2003). Postseismic Fault healing on the rupture zone of the 1999 M 7.1 Hector Mine, California, Earthquake. *Bulletin of the Seismological Society of America*, 93(2), 854–869. <https://doi.org/10.1785/0120020131>
- Lyakhovskiy, V., Ben-Zion, Y., & Agnon, A. (2005). A viscoelastic damage rheology and rate- and state-dependent friction. *Geophysical Journal International*, 161(1), 179–190. <https://doi.org/10.1111/j.1365-246x.2005.02583.x>
- McFarland, F. S., Lienkaemper, J. J., & Caskey, S. J. (2009). *Data from theodolite measurements of creep rates on San Francisco Bay region faults, California, 1979-2012 (USGS Numbered Series No. 2009-1119)*. U.S. Geological Survey. (Code Number: 2009-1119 Code: Data from theodolite measurements of creep rates on San Francisco Bay region faults, California, 1979-2012 Publication Title: Data from theodolite measurements of creep rates on San Francisco Bay region faults, California, 1979-2012 Reporter: Data from theodolite measurements of creep rates on San Francisco Bay region faults, California, 1979-2012 Series: Open-File Report). <https://doi.org/10.3133/ofr20091119>
- Mizuno, T., Kuwahara, Y., Ito, H., & Nishigami, K. (2008). Spatial variations in fault-zone structure along the Nojima fault, central Japan, as inferred from borehole observations of fault-zone trapped waves. *Bulletin of the Seismological Society of America*, 98(2), 558–570. <https://doi.org/10.1785/0120060247>
- Murray, J. R., Minson, S. E., & Svarc, J. L. (2014). Slip rates and spatially variable creep on faults of the northern San Andreas system inferred through Bayesian inversion of Global Positioning System data. *Journal of Geophysical Research: Solid Earth*, 119(7), 6023–6047. <https://doi.org/10.1002/2014JB010966>
- Okubo, K., Bhat, H. S., Rougier, E., Marty, S., Schubnel, A., Lei, Z., & Klinger, Y. (2019). Dynamics, radiation, and overall energy budget of earthquake rupture with coseismic off-fault damage. *Journal of Geophysical Research: Solid Earth*.
- Pei, S., Niu, F., Ben-Zion, Y., Sun, Q., Liu, Y., Xue, X., et al. (2019). Seismic velocity reduction and accelerated recovery due to earthquakes on the Longmenshan fault. *Nature Geoscience*, 12(5), 387–392. <https://doi.org/10.1038/s41561-019-0347-1>
- Peng, Z., & Ben-Zion, Y. (2006). Temporal changes of shallow seismic velocity around the Karadere-Düzce Branch of the North Anatolian Fault and strong ground motion. *Pure and Applied Geophysics*, 163(2), 567–600. <https://doi.org/10.1007/s00024-005-0034-6>
- Perrin, C., Manighetti, I., Ampuero, J.-P., Cappa, F., & Gaudemer, Y. (2016). Location of largest earthquake slip and fast rupture controlled by along-strike change in fault structural maturity due to fault growth. *Journal of Geophysical Research: Solid Earth*, 121(5), 3666–3685. <https://doi.org/10.1002/2015JB012671>
- Rice, J. R. (1993). Spatio-temporal complexity of slip on a fault. *Journal of Geophysical Research*, 98(B6), 9885–9907. <https://doi.org/10.1029/93jb00191>
- Rice, J. R., & Ben-Zion, Y. (1996). Slip complexity in earthquake fault models. *Proceedings of the National Academy of Sciences*, 93(9), 3811–3818. <https://doi.org/10.1073/pnas.93.9.3811>
- Roux, P., & Ben-Zion, Y. (2014). Monitoring fault zone environments with correlations of earthquake waveforms. *Geophysical Journal International*, 196(2), 1073–1081. <https://doi.org/10.1093/gji/ggt441>
- Rubinstein, J. L., & Beroza, G. C. (2005). Depth constraints on nonlinear strong ground motion from the 2004 Parkfield earthquake. *Geophysical Research Letters*, 32(14). <https://doi.org/10.1029/2005gl023189>
- Ruina, A. (1983). Slip instability and state variable friction laws. *Journal of Geophysical Research*, 88(B12), 10359–10370. <https://doi.org/10.1029/JB088B12p10359>

- Scholz, C. H. (1998). Earthquakes and friction laws. *Nature*, 391(6662), 37–42. <https://doi.org/10.1038/34097>
- Snieder, R., Sens-Schönfelder, C., Ruigrok, E., & Shiomi, K. (2016). Seismic shear waves as Foucault pendulum. *Geophysical Research Letters*, 43(6), 2576–2581. <https://doi.org/10.1002/2015gl067598>
- Taira, T., Silver, P. G., Niu, F., & Nadeau, R. M. (2009). Remote triggering of fault-strength changes on the San Andreas Fault at Parkfield. *Nature*, 461(7264), 636–639. <https://doi.org/10.1038/nature08395>
- Thakur, P., Huang, Y., & Kaneko, Y. (2020). Effects of low-velocity fault damage zones on long-term earthquake behaviors on mature strike-slip faults. *Journal of Geophysical Research: Solid Earth*, 125(8). <https://doi.org/10.1029/2020JB019587>
- Tong, X., Sandwell, D. T., & Smith-Konter, B. (2013). High-resolution interseismic velocity data along the San Andreas Fault from GPS and InSAR. *Journal of Geophysical Research: Solid Earth*, 118(1), 369–389. <https://doi.org/10.1029/2012JB009442>
- Tsai, V. C., & Hirth, G. (2020). Elastic impact consequences for high-frequency earthquake ground motion. *Geophysical Research Letters*, 47(5), e2019GL086302. <https://doi.org/10.1029/2019gl086302>
- Vidale, J. E., & Li, Y.-G. (2003). Damage to the shallow Landers fault from the nearby Hector Mine earthquake. *Nature*, 421(6922), 524–526. <https://doi.org/10.1038/nature01354>
- Waldhauser, F., & Ellsworth, W. L. (2002). Fault structure and mechanics of the Hayward fault, California, from double-difference earthquake locations. *Journal of Geophysical Research*, 107(B3). <https://doi.org/10.1029/2000jb000084>
- Wang, K., & Bilek, S. L. (2014). Invited review paper: Fault creep caused by subduction of rough seafloor relief. *Tectonophysics*, 610, 1–24. <https://doi.org/10.1016/j.tecto.2013.11.024>
- Wu, C., Peng, Z., & Ben-Zion, Y. (2009). Non-linearity and temporal changes of fault zone site response associated with strong ground motion. *Geophysical Journal International*, 176(1), 265–278. <https://doi.org/10.1111/j.1365-246X.2008.04005.x>
- Zhao, P., & Peng, Z. (2009). Depth extent of damage zones around the Central Calaveras fault from waveform analysis of repeating earthquakes. *Geophysical Journal International*, 179(3), 1817–1830. <https://doi.org/10.1111/j.1365-246x.2009.04385.x>

References From the Supporting Information

- Barbot, S. (2019a). Modulation of fault strength during the seismic cycle by grain-size evolution around contact junctions. *Tectonophysics*, 765, 129–145. <https://doi.org/10.1016/j.tecto.2019.05.004>
- Blanpied, M., Lockner, D., & Byerlee, J. (1991). Fault stability inferred from granite sliding experiments at hydrothermal conditions. *Geophysical Research Letters*, 18(4), 609–612. <https://doi.org/10.1029/91gl00469>
- Cattania, C. (2019). Complex earthquake sequences on simple faults. *Geophysical Research Letters*, 46(17–18), 10384–10393. <https://doi.org/10.1029/2019gl083628>
- Dieterich, J. H. (1979). Modeling of rock friction: 1. Experimental results and constitutive equations. *Journal of Geophysical Research*, 84(B5), 2161–2168. <https://doi.org/10.1029/JB084iB05p02161>
- Erickson, B. A., Jiang, J., Barall, M., Lapusta, N., Dunham, E. M., Harris, R., et al. (2020). The community code verification exercise for simulating sequences of earthquakes and aseismic slip (SEAS). *Seismological Research Letters*, 91(2A), 874–890. <https://doi.org/10.1785/0220190248>
- Kaneko, Y., Ampuero, J.-P., & Lapusta, N. (2011). Spectral-element simulations of long-term fault slip: Effect of low-rigidity layers on earthquake-cycle dynamics. *Journal of Geophysical Research*, 116, B10313. <https://doi.org/10.1029/2011JB008395>
- Kaneko, Y., Lapusta, N., & Ampuero, J.-P. (2008). Spectral element modeling of spontaneous earthquake rupture on rate and state faults: Effect of velocity-strengthening friction at shallow depths. *Journal of Geophysical Research*, 113(B9). <https://doi.org/10.1029/2007jb005553>
- Lapusta, N., & Rice, J. R. (2003). Nucleation and early seismic propagation of small and large events in a crustal earthquake model. *Journal of Geophysical Research*, 108(B4). <https://doi.org/10.1029/2001jb000793>
- Lapusta, N., Rice, J. R., Ben-Zion, Y., & Zheng, G. (2000). Elastodynamic analysis for slow tectonic loading with spontaneous rupture episodes on faults with rate- and state-dependent friction. *Journal of Geophysical Research*, 105(B10), 23765–23789. <https://doi.org/10.1029/2000JB900250>